Science of the Total Environment 433 (2012) 216–229

Contents lists available at SciVerse ScienceDirect

Science of the Total Environment

journal homepage: www.elsevier.com/locate/scitotenv

Bioavailable $^{87}Sr/^{86}Sr$ in different environmental samples — Effects of anthropogenic contamination and implications for isoscapes in past migration studies

Anne-France Maurer [a,*], Stephen J.G. Galer [b], Corina Knipper [c], Lars Beierlein [d], Elizabeth V. Nunn [a], Daniel Peters [e], Thomas Tütken [f], Kurt W. Alt [c], Bernd R. Schöne [a]

[a] Earth System Science Research Center, Department of Applied and Analytical Paleontology, Institute of Geosciences, University of Mainz, Johann-Joachim-Becher-Weg 21, 55128 Mainz, Germany
[b] Max Planck Institute for Chemistry, Department of Biogeochemistry, Johann-Joachim-Becher-Weg 27, 55128 Mainz, Germany
[c] Institute of Anthropology, University of Mainz, Colonel-Kleinmann-Weg 2, 55128 Mainz, Germany
[d] Alfred Wegener Institute for Polar and Marine Research, Am Handelshafen 12, 27570 Bremerhaven, Germany
[e] Roman-Germanic-Commission, Palmengartenstraße 10–12, 60325 Frankfurt/M., Germany
[f] Steinmann-Institute for Geology, Mineralogy and Paleontology, Poppelsdorfer Schloss, University of Bonn, 53115 Bonn, Germany

A R T I C L E I N F O

Article history:
Received 31 March 2012
Received in revised form 13 June 2012
Accepted 13 June 2012
Available online 13 July 2012

Keywords:
Strontium isotopes
Anthropogenic contamination
Environmental samples
Human teeth
Past migration

A B S T R A C T

$^{87}Sr/^{86}Sr$ reference maps (isoscapes) are a key tool for investigating past human and animal migrations. However, there is little understanding of which biosphere samples are best proxies for local bioavailable Sr when dealing with movements of past populations. In this study, biological and geological samples (ground vegetation, tree leaves, rock leachates, water, soil extracts, as well as modern and archeological animal teeth and snail shells) were collected in the vicinity of two early medieval cemeteries ("Thuringians", 5–6th century AD) in central Germany, in order to characterize $^{87}Sr/^{86}Sr$ of the local biosphere. Animal tooth enamel is not appropriate in this specific context to provide a reliable $^{87}Sr/^{86}Sr$ baseline for investigating past human migration. Archeological faunal teeth data (pig, sheep/goat, and cattle) indicates a different feeding area compared to that of the human population and modern deer teeth $^{87}Sr/^{86}Sr$ suggest the influence of chemical fertilizers. Soil leachates do not yield consistent $^{87}Sr/^{86}Sr$, and $^{87}Sr/^{86}Sr$ of snail shells are biased towards values for soil carbonates. In contrast, water and vegetation samples seem to provide the most accurate estimates of bioavailable $^{87}Sr/^{86}Sr$ to generate Sr isoscapes in the study area. Long-term environmental archives of bioavailable $^{87}Sr/^{86}Sr$ such as freshwater bivalve shells and tree cores were examined in order to track potential historic anthropogenic contamination of the water and the vegetation. The data obtained from the archeological bivalve shells show that the modern rivers yield $^{87}Sr/^{86}Sr$ ratios which are similar to those of the past. However, the tree cores registered decreasing $^{87}Sr/^{86}Sr$ values over time towards present day likely mirroring anthropogenic activities such as forest liming, coal mining and/or soil acidification. The comparison of $^{87}Sr/^{86}Sr$ of the Thuringian skeletons excavated in the same area also shows that the vegetation samples are very likely anthropogenically influenced to some extent, affecting especially $^{87}Sr/^{86}Sr$ of the shallow rooted plants.

1. Introduction

Over the past decade, strontium (Sr) isotope analysis has become an increasingly powerful tool in present-day and past animal ecology, for determining habitat use and mobility/migration (Blum et al., 2001; Britton et al., 2011; Feranec et al., 2007; Hoppe et al., 1999; Hoppe and Koch, 2007; Radloff et al., 2010; Tütken et al., 2011), in tracing food provenance (Almeida and Vasconcelos, 2001; Barbaste et al., 2002; Fortunato et al., 2004; Montgomery et al., 2006; Swoboda et al., 2008; Techer et al., 2011; Voerkelius et al., 2010), in hydrological and forest ecosystem investigations (Böhlke and Horan, 2000; Dijkstra et al., 2003; Drouet et al., 2005b, 2007; Poszwa et al., 2004; Shand et al., 2009), as well as in forensic sciences (Beard and Johnson, 2000; Juarez, 2008).

In archeology, the Sr isotopic composition can be used to identify migrants and to examine movements of individuals (Bentley et al., 2002, 2003; Knudson et al., 2004, 2005; Kusaka et al., 2011; Montgomery et al., 2007; Müller et al., 2003; Price et al., 2000, 2006a, 2006b; Schweissing and Grupe, 2003; Tafuri et al., 2006; Tung and Knudson, 2008; Wright, 2005). Such information, in turn, provides insight into the dynamics and economy of past populations.

Strontium has four stable isotopes (^{88}Sr, ^{87}Sr, ^{86}Sr and ^{84}Sr) of which ^{87}Sr is radiogenic, resulting from the long-lived radioactive decay of ^{87}Rb, and is therefore variable in nature. The $^{87}Sr/^{86}Sr$ ratio

* Corresponding author.
E-mail address: annefrance.maurer@gmail.com (A-F. Maurer).

0048-9697/$ – see front matter
doi:10.1016/j.scitotenv.2012.06.046

of a closed system is controlled by the initial $^{87}Sr/^{86}Sr$ ratio, the Rb/Sr ratio and time elapsed (Dasch, 1969). Different geological substrates therefore possess varying $^{87}Sr/^{86}Sr$ ratios according to the Sr-bearing minerals that they contain and their geological age. Weathering of the bedrock material releases Sr from minerals, which then percolates through soil pore waters and into the ecosystem (Ericson, 1985; Graustein, 1989). Strontium has similar chemical properties to calcium and tends to follow the same biological pathways; however, there is preferential absorption and retention of Ca over Sr by organisms (Comar et al., 1957). Strontium is mostly absorbed via drinking water and diet, in relative proportions to the Ca content in the foodstuffs, and is mainly stored in vertebrates in the mineral phases of bones and teeth (Comar et al., 1957; Rosenthal et al., 1972; Toots and Voorhies, 1965). Consequently, the skeletal $^{87}Sr/^{86}Sr$ mirrors, in a complex way, that of underlying geological strata (Ericson, 1985).

Because $^{87}Sr/^{86}Sr$ is inherited from the local environment, residential mobility and lifestyle of individuals, or whole populations, can be evaluated using the Sr isotope signatures of skeletal tissues. To do so and, for example, to identify potential non-local individuals, it is necessary to define the so-called "local" bioavailable $^{87}Sr/^{86}Sr$ signature, which is a challenging task (Bentley et al., 2004; Price et al., 2002; Tütken et al., 2011). A variety of comparative sample materials have been used in this regard, each of which has advantages and disadvantages (Evans and Tatham, 2004). The enamel of archeological faunal teeth from a site are one of the best indicators of the local range (Price et al., 2002), but their exact origin may be questionable. Modern faunal samples from known localities can also provide estimates of the local biologically-available $^{87}Sr/^{86}Sr$. Different environmental samples have been put forward to assess the spatial variability in the bioavailable $^{87}Sr/^{86}Sr$. These include surface water, soil leachates, vegetation and snail shells (Evans et al., 2010; Hodell et al., 2004; Nafplioti, 2011; Price et al., 2002; Sillen et al., 1998). However, industrial/anthropogenic activities, such as the use of fertilizers, might have influenced the Sr isotope ratios of modern ecosystems (Böhlke and Horan, 2000; Christian et al., 2011; Tichomirowa et al., 2010; West et al., 2009), which would then be inappropriate for interpreting $^{87}Sr/^{86}Sr$ data of archeological specimens.

A prerequisite for investigating past human migration is the understanding of the Sr catchment area of the comparative samples used to characterize the $^{87}Sr/^{86}Sr$ ratio of the bioavailable Sr. In this study, different kinds of samples were tested (modern deer enamel, water, soil and rock leachates, snail shells and vegetation) in order to identify where they get their Sr from, and to determine whether or not they are suitable as reference samples to investigate past human migration in central Europe. Additional analyses of environmental samples, such as modern and archeological freshwater bivalve shells, as well as modern tree cores (Åberg, 1995) were performed in order to monitor potential changes in bioavailable ecosystem $^{87}Sr/^{86}Sr$ over time. Finally the $^{87}Sr/^{86}Sr$ results obtained from the modern ecosystem were compared to $^{87}Sr/^{86}Sr$ measured in archeological human teeth excavated in the same area (so-called "Thuringians", 5–6th century AD, Saxony-Anhalt, Germany; see Knipper et al., 2012).

2. Geological settings

The environmental investigation focuses mainly around the early medieval cemeteries of Obermöllern and Rathewitz in the SW of the German federal state of Saxony-Anhalt (Fig. 1). The archeological settings of these cemeteries have been outlined in Knipper et al. (2012). Within a 50 km radius surrounding the archeological cemeteries, the geology consists of Permian to Quaternary sedimentary rocks.

A review of the geology can be found in Ziegler (1990). Permian Zechstein evaporates (sulfates and halite) and carbonates, are found south of the Harz Mountains and north of the Thuringian Highlands, which are two Paleozoic geological units crosscut by plutonic and volcanic intrusions. Zechstein deposits are absent close to the cemeteries; however, they run alongside the Helme River and are found in the northern part of the Saale River, from which the freshwater bivalve shells were collected as part of this study. The two Paleozoic bedrock highs constitute the northern and southern borders of the Thuringian Basin, mainly underlain by the Triassic Buntsandstein, Muschelkalk and Keuper units. The Buntsandstein comprises three distinct facies: Lower Buntsandstein (shaley sediments), Middle Buntsandstein (sandstones and shales) and Upper Buntsandstein composed of shales and evaporates (Nollet et al., 2009; Ziegler, 1990). The Muschelkalk is mostly composed of carbonates and marls, while the Keuper is formed by clastic–evaporitic deposits of intercalated clays, sandstones, salts and dolomite. The archeological cemeteries, located on the eastern edge of the basin, are surrounded by residual Triassic deposits. Small Oligocene units (sand and clay) are also found near the necropoleis. Tertiary deposits become more preponderant further east, accompanied by glacial and periglacial Quaternary sediments, which form the main surface cover of north and north-eastern Germany. Loess deposits also cover large proportions of the surface of the study area.

3. Material and methods

3.1. Sample collection

Strontium isotope analyses of 155 biological and geological samples were undertaken in this study (Tables 1 and 2). Most of the samples were collected in April 2009, from 50 locations in the vicinity of the two "Thuringian" cemeteries, and mostly within a 4 km radius around them (Fig. 2). In order to avoid contamination by fertilizers, samples were taken from forests and quarries covering the major geological units of the area. Sampling locations were recorded by a hand-held GPS device.

The samples consist of rocks, soils, snail shells and plants, collected at the same locations if possible (Table 1). Two kinds of plant samples were considered: ground vegetation (mainly grass) and tree leaves (Beech, Maple, Oak, Lime and Hazel). Fresh leaves were taken from the same tree and/or from grass. A few grams of soil were collected from the uppermost 15 cm of the mineral soil after removing the humus layer, which should correspond closely to that of the exchangeable cation pool (Blum et al., 2000; Pett-Ridge et al., 2009). Rock samples and snail shells (*Helix pomatia*, except for locality No. 3, *Cepaea hortensis*) were obtained as well, and close to the plant samples whenever possible. All of the samples were stored in zip-lock plastic bags.

In order to complement the collection, some additional samples from the same overall area were obtained:

- Twelve water samples from rivers and springs (w1–12; Table 2), were sampled using a syringe and stored in 30 ml acid-cleaned Teflon tubes, acidified with 100 µl HNO_3. Samples were stored for less than a month in a refrigerator prior to analysis.
- Two soil samples: one soil core, obtained with a soil core sampler and reaching a depth of 60 cm (Table 1; locality No. 8), and one soil (as well as cereal) sampled directly from an agricultural field (Table 1; locality No. 10), were collected in order to specifically assess the impact of fertilizer use in this region on the $^{87}Sr/^{86}Sr$.
- Two tree cores from oaks nearby each cemetery were obtained using an increment borer (Table 2) to look for possible variations in the bioavailable $^{87}Sr/^{86}Sr$ over the last century (from 1925 to 2003; sampling resolution: five years).
- Nine modern roe deer teeth (Table 2) from road killed animals (localities of Steinburg, Wallroda, Kalbitz and Steinbach), were provided by the Forestry Office of Sachsen-Anhalt.
- Faunal tooth enamel from eleven animals (8 pigs, 2 cattle, 1 sheep/goat; Table 2) were obtained from the archeological cemeteries of Obermöllern (Thuringian and Iron Age), Eulau (Iron Age)

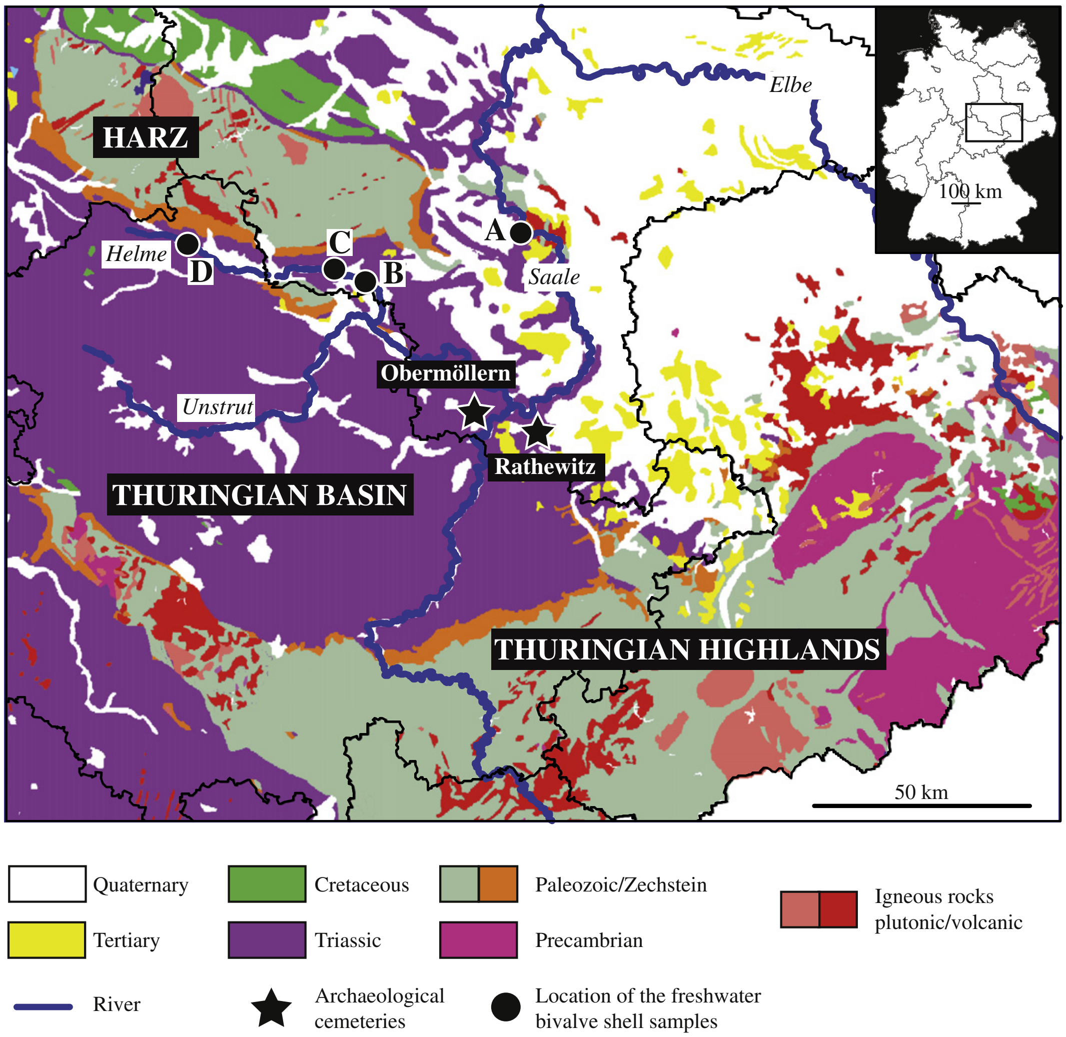

Fig. 1. Geological map of the study area (modified from GK1000, BGR Geologie) showing the location of the archeological cemeteries (Obermöllern and Rathewitz), and the freshwater bivalve shell sampling locations (A to D).

and Schönburg (Iron Age), for use as pre-anthropogenic reference material (locations, see Fig. 2).

- Seven freshwater bivalve shells (Unionidae) from four locations (A to D; Fig. 1), approximately 5 to 20 years old, were investigated (Table 2) to examine potential temporal variations in the bioavailable $^{87}Sr/^{86}Sr$ from river waters. Two modern specimens (collected in 1997 and 2009) and five archeological specimens (excavated in cemeteries dating from the middle Neolithic Salzmünde culture to the old Iron Age) were analyzed. The rivers (Saale and Helme) were sampled during the spring of 2010. These water samples were taken 50 to 100 km north of the cemeteries, at the southern border of the Harz Mountains (Fig. 1).

3.2. Sample preparation and analysis

Leaves and snail shells were rinsed with demineralized water soon after collection, and dried overnight at 50 °C. Approximately 1 g of dried leaves was ground manually and ashed in acid-washed silica crucibles at 550 °C for 12 h. Six tree ring samples of 80 to 150 mg, averaging 5 years each, were taken from both tree cores, covering a time span from 1925 to 2003. A surgical steel scalpel was used to take the samples from the core and to clean their surfaces. They were then ashed in a muffle furnace at 250 °C for 2 h, followed by manual grinding with an agate pestle and mortar. The surfaces of the snail shells and that of the faunal tooth enamel (modern and archeological) were mechanically cleaned using a drill diamond bit. A fraction of the snail shells (3–5 mg) was then ground with an agate mortar, while 10 mg of faunal tooth enamel was directly collected with the drill. The archeological faunal enamel samples were treated with pH = 4.5 buffer solution (0.1 M Li acetate–acetic acid solution) to remove any diagenetic carbonate precipitated during burial. The bivalve shells were embedded in epoxy resin, cut perpendicular to the direction of growth, ground and polished. Between 0.3 and 0.9 mg of shell powder from the early and the late ontogenetic years (averaging 2 to 3 years each) was obtained by micromilling according to the protocol described in Hallmann et al. (2008) with a diamond-coated cylindrical drill bit of 1 mm diameter. The soil leachates were obtained by shaking 1 g of soil in 10 ml MilliQ (Millipore) water for 24 h in acid-cleaned polypropylene tubes. This step was followed by 1 h in an ultrasonic bath. The resulting solution was filtered through 0.2 μm filters before being dried down. The powder obtained from the rocks with a diamond-coated drill bit was leached with water as well. After decantation, 2 ml of the water collected from rivers and springs was sampled and dried down.

The major portion of the samples was analyzed at the Max Planck Institute for Chemistry in Mainz, Germany. All samples were dissolved in sub-boiling distilled hydrochloric acid (snail and bivalve shells) or nitric acid (enamel and vegetation, with the addition of 30% H_2O_2), respectively, and evaporated to dryness. The strontium fraction was separated from the samples using Sr-SPEC Eichrom

Table 1
Strontium isotope ratios of modern environmental samples (rock and soil leachates, snail shells, ground vegetation and tree leaves) collected from 39 locations in the vicinity of two Thuringian cemeteries (Obermöllern and Rathewitz) and sorted according to the geological substrate (Buntsandstein: Middle and Upper; Muschelkalk: Lower and Middle; Keuper, Oligocene, Pleistocene and Holocene). Locality No. 21 provided samples from a Muschelkalk quarry as well as from the Pleistocene sediments covering the Muschelkalk. Samples in italics are not included in statistical calculations because of potential anthropogenic contamination effects.

Locality no.	Type of sample location	Latitude	Longitude	Epoch	Rock	Soil	Snail	Ground vegetation		Tree leave	
					$^{87}Sr/^{86}Sr \pm 2\sigma$	$^{87}Sr/^{86}Sr \pm 2\sigma$	$^{87}Sr/^{86}Sr \pm 2\sigma$	$^{87}Sr/^{86}Sr \pm 2\sigma$	Common name	$^{87}Sr/^{86}Sr \pm 2\sigma$	Common name
1	Alluvial plain	51.11822	11.85434	Holocene				0.70820 ± 0.00005[a]	Grass		
2	Forest	51.15312	11.76641	Holocene			0.70905 ± 0.00001	0.70864 ± 0.00001	Grass	0.70897 ± 0.00001	Oak
3	Alluvial plain	51.22667	11.67986	Holocene			0.70840 ± 0.00004	0.70842 ± 0.00003[a]	Grass		
4	Forest	51.16321	11.66920	Pleistocene			*0.70811 ± 0.00001*	0.70892 ± 0.00001[a]	Grass	0.70945 ± 0.00001	Maple
5	Forest	51.16136	11.66185	Pleistocene				0.70950 ± 0.00001[a]	Anemone	0.70966 ± 0.00001	Maple
6	Forest	51.16371	11.66361	Pleistocene				0.70949 ± 0.00004[a]	Anemone	0.70976 ± 0.00004	Beech
7	Quarry loess	51.12470	11.86896	Pleistocene			0.70910 ± 0.00001	0.70972 ± 0.00001[a]	Grass		
8	Forest	51.11538	11.87961	Pleistocene		0.71012 ± 0.00002	0.70861 ± 0.00001	0.70898 ± 0.00001[a]	Greater celandine	0.70939 ± 0.00001	Hazel
						Soil core	[Depth cm]			0.70935 ± 0.00002	Oak
						0.70884 ± 0.00002	[15]				
						0.71237 ± 0.00002	[30]				
						0.71169 ± 0.00002	[45]				
						0.71478 ± 0.00002	[60]				
9	Forest	51.11224	11.89450	Pleistocene		*0.70772 ± 0.00002*		*0.70776 ± 0.00004*[a]	*Grass*	*0.70791 ± 0.00002*	*Maple*
10	Agricultural field	51.16241	11.66505	Pleistocene		0.70553 ± 0.00001		0.70551 ± 0.00001[a]	Cereal		
11	Forest	51.16140	11.66401	Pleistocene		0.70958 ± 0.00001		0.70936 ± 0.00001	Anemone	0.70983 ± 0.00001	Lime tree
21	Quarry Muschelkalk	51.16584	11.66751	Pleistocene		0.71054 ± 0.00007		0.71016 ± 0.00001	Grass		
								0.71027 ± 0.00001	Lotus		
12	Forest	51.15581	11.72055	Oligocene		0.70931 ± 0.00002		0.70933 ± 0.00008[a]	Anemone	0.70942 ± 0.00001	Beech
13	Forest	51.15433	11.72152	Oligocene				0.70887 ± 0.00002[a]	Grass		
14	Forest	51.15279	11.72165	Oligocene				0.70959 ± 0.00001[a]	Grass	0.70959 ± 0.00001	Oak
15	Forest	51.12938	11.53619	Keuper						0.70964 ± 0.00001	Beech
16	Forest	51.13093	11.53640	Muschelkalk (Middle)						0.70925 ± 0.00006	Beech
17	Forest	51.13065	11.53562	Muschelkalk (Middle)	0.70811 ± 0.00006		0.70905 ± 0.00003			0.70913 ± 0.00001	Beech
					0.70822 ± 0.00007						
18	Forest	51.16557	11.67017	Muschelkalk (Lower)			0.70836 ± 0.00003				
19	Forest	51.16552	11.66985	Muschelkalk (Lower)			0.70839 ± 0.00003				
20	Forest	51.16552	11.66983	Muschelkalk (Lower)				0.70819 ± 0.00003	Grass		
21	Quarry Muschelkalk	51.16584	11.66751	Muschelkalk (Lower)	0.70784 ± 0.00004		0.70848 ± 0.00001				
22	Quarry Muschelkalk	51.16572	11.66749	Muschelkalk (Lower)	0.70782 ± 0.00005			0.70866 ± 0.00006[a]	Grass		
23	Quarry Muschelkalk	51.16591	11.66681	Muschelkalk (Lower)	0.70783 ± 0.00003			0.70875 ± 0.00004[a]	Grass		
24	Forest	51.16388	11.66423	Muschelkalk (Lower)			0.70871 ± 0.00001				
25	Quarry Muschelkalk	51.16465	11.66454	Muschelkalk (Lower)	0.70796 ± 0.00001		0.70863 ± 0.00004	0.70840 ± 0.00006	Woodruff		
26	Forest	51.16455	11.66473	Muschelkalk (Lower)			0.70831 ± 0.00001				
27	Forest	51.15637	11.64908	Muschelkalk (Lower)				0.70866 ± 0.00002[a]	Ivy		
28	Forest	51.15689	11.64857	Muschelkalk (Lower)			0.70838 ± 0.00004	0.70875 ± 0.00002[a]	Grass	0.70910 ± 0.00012	Beech
										0.70900 ± 0.00001	Beech
29	Forest	51.12333	11.86359	Muschelkalk (Lower)			0.70783 ± 0.00003			0.70817 ± 0.00004	Lime tree
30	Forest	51.12321	11.86382	Muschelkalk (Lower)			0.70797 ± 0.00006	0.70855 ± 0.00002[a]	Grass	0.70884 ± 0.00006	Maple
31	Forest	51.12322	11.86339	Muschelkalk (Lower)	0.70803 ± 0.00018		0.70822 ± 0.00001	0.70824 ± 0.00001[a]	Ivy-leaved speedwell	0.70836 ± 0.00001	Oak
32	Forest	51.12475	11.85100	Muschelkalk (Lower)			0.70798 ± 0.00005	0.70827 ± 0.00003[a]	Wild ginger	0.70839 ± 0.00012	Beech
33	Forest	51.13501	11.84944	Buntsandstein (Upper)	0.70838 ± 0.00002		0.70857 ± 0.00003	0.70858 ± 0.00001[a]	Anemone	0.70920 ± 0.00010	Lime tree
34	Forest	51.13533	11.84760	Buntsandstein (Upper)						0.71016 ± 0.00003	Beech
35	Forest	51.13544	11.84785	Buntsandstein (Upper)			0.70977 ± 0.00001	0.70950 ± 0.00001[a]	Unknown		
36	Forest	51.13485	11.84518	Buntsandstein (Upper)	0.71004 ± 0.00001			0.70975 ± 0.00001[a]	Anemone	0.71008 ± 0.00001	Beech
37	Forest	51.19076	11.52319	Buntsandstein (Middle)		0.71213 ± 0.00002		0.71060 ± 0.00001[a]	Grass	0.71074 ± 0.00001	Beech
38	Forest	51.19070	11.52306	Buntsandstein (Middle)						0.71116 ± 0.00005	Hazel
39	Forest	51.19076	11.52169	Buntsandstein (Middle)			0.70959 ± 0.00001				

[a] Already published in Knipper et al., 2012.

Table 2
Additional environmental $^{87}Sr/^{86}Sr$ data from tree cores, freshwater bivalve shells, water samples, modern deer tooth enamel and archeological faunal tooth enamel samples. The $^{87}Sr/^{86}Sr$ of Thuringian human skeletons from 5 to 6th century AD from Obermöllern and Rathewitz cemeteries (Knipper et al., 2012) are also reported.

Locality	Latitude	Longitude	Sample		$^{87}Sr/^{86}Sr \pm 2\sigma$
Tree core samples					
Near Obermöllern	51.16363	11.66350	Years 1925–1930		0.71005 ± 0.00001
			Years 1940–1945		0.70989 ± 0.00005
			Years 1960–1965		0.70930 ± 0.00005
			Years 1970–1975		0.71025 ± 0.00001
			Years 1985–1990		0.70927 ± 0.00002
			Years 1998–2003		0.70922 ± 0.00001
Near Rathewitz	51.11563	11.87962	Years 1925–1930		0.71097 ± 0.00001
			Years 1940–1945		0.71041 ± 0.00001
			Years 1960–1965		0.70968 ± 0.00001
			Years 1970–1975		0.70936 ± 0.00001
			Years 1985–1990		0.70942 ± 0.00001
			Years 1998–2003		0.70935 ± 0.00002
Freshwater bivalve shells					
A. (Saale River)	51.53495	11.81891	1. Middle Neolithic (early ontogeny)		0.70833 ± 0.00001
			1. Middle Neolithic (late ontogeny)		0.70835 ± 0.00001
			2. Middle Neolithic (early ontogeny)		0.70840 ± 0.00001
			2. Middle Neolithic (late ontogeny)		0.70836 ± 0.00001
			3. Early Bronze Age (early ontogeny)		0.70841 ± 0.00001
			3. Early Bronze Age (late ontogeny)		0.70841 ± 0.00001
			4. Late Bronze Age/pre-Roman Iron Age (early ontogeny)		0.70845 ± 0.00001
B. (Helme River)	51.43190	11.30399	5. Old Iron Age		0.70821 ± 0.00001
C. (Helme River)	51.45697	11.20076	6. Died in 1997/1998 (early ontogeny)		0.70798 ± 0.00001
			6. Died in 1997/1998 (late ontogeny)		0.70789 ± 0.00001
D. (Helme River)	51.50400	10.70887	7. Died in 2009 (early ontogeny)		0.71001 ± 0.00001
			7. Died in 2009 (late ontogeny)		0.70999 ± 0.00001
Water samples				Sr content $\mu g.l^{-1}$	
w1	51.19088	11.52330	Steinbach River	306	0.71011 ± 0.00024[a]
w2	51.19057	11.52309	Steinbach River	309	0.71026 ± 0.00017[a]
w3	51.19070	11.52306	Spring	319	0.71051 ± 0.00012[a]
w4	51.19193	11.73039	Hasselbach River	1088	0.70913 ± 0.00020[a]
w5	51.16111	11.64105	Hasselbach River	1495	0.70919 ± 0.00023[a]
w6	51.12456	11.85215	Spring	1318	0.70919 ± 0.00001[a]
w7	51.12005	11.87561	Spring	482	0.71064 ± 0.00017[a]
w8	51.11808	11.85450	Wethau River	772	0.70960 ± 0.00027[a]
w9	51.12301	11.87309	Schoppbach River	492	0.71011 ± 0.00005[a]
w10	51.13588	11.86652	Nautsche River	449	0.71040 ± 0.00012[a]
w11	51.22633	11.67894	Unstrut River	2822	0.70845 ± 0.00010[a]
w12	51.15250	11.76591	Saale River	889	0.70887 ± 0.00013[a]
w13	51.53115	11.82333	Saale River	1443	0.70867 ± 0.00001
w14	51.52952	10.48907	Helme River	284	0.71178 ± 0.00001
w15	51.50860	10.69175	Helme River	457	0.70977 ± 0.00001
w16	51.44870	11.20250	Helme River	754	0.70801 ± 0.00001
w17	51.43151	11.30529	Helme River	802	0.70811 ± 0.00001
w18	51.45226	11.19619	Helme River	654	0.70804 ± 0.00001
Modern deer tooth enamel					
Steinburg	51.19069	11.51780	Second molar		0.70933 ± 0.00001
Wallroda	51.19693	11.54340	Third molar		0.70734 ± 0.00001
			Third molar		0.70730 ± 0.00001
Kalbitz	51.19106	11.55949	Third molar		0.70792 ± 0.00001
Steinbach	51.19044	11.58284	Third molar		0.70703 ± 0.00001
			Third molar		0.70800 ± 0.00001
			Third molar		0.70666 ± 0.00001
			Third molar		0.70713 ± 0.00001
			Third molar		0.70788 ± 0.00001
Archeological faunal tooth enamel					
Eulau Iron Age	51.16475	11.84572	Pig: second molar		0.70912 ± 0.00001
			Pig: deciduous molar		0.70927 ± 0.00001
			Pig: first molar		0.70930 ± 0.00001
			Pig: second molar		0.70901 ± 0.00001
Obermöllern Iron Age	51.16235	11.66984	Pig: first molar		0.70886 ± 0.00001[a]
			Sheep/goat: third molar		0.70964 ± 0.00001[a]
			Cattle: deciduous molar		0.70954 ± 0.00001[a]
			Cattle: third molar		0.71297 ± 0.00001
Obermöllern Thuringian	51.16235	11.66984	Pig: third molar		0.71046 ± 0.00033[a]
Schönburg Iron Age	51.17397	11.88019	Pig: third molar		0.70943 ± 0.00001
			Pig: third molar		0.71204 ± 0.00001
Human bones (average calculated from data published in Knipper et al., 2012)					

Table 2 (*continued*)

Locality	Latitude	Longitude	Sample	$^{87}Sr/^{86}Sr \pm 2\sigma$
Obermöllern	51.16235	11.66984		0.70976 ± 0.00046
Rathewitz	51.12126	11.87862		0.71004 ± 0.00061
Human teeth (average calculated from data published in Knipper et al., 2012)				
Obermöllern	51.16235	11.66984		0.71021 ± 0.00234
Rathewitz	51.12126	11.87862		0.71000 ± 0.00233

[a] Already published in Knipper et al., 2012.

resin. Approximately, 100 ng of purified Sr was loaded onto tungsten filaments with Ta-fluoride activator. Strontium isotopic compositions were measured using a Triton (ThermoFisher) TIMS instrument. The standard reference material NIST SRM 987 yielded 0.710270 ± 10 (1σ, population) for 41 measurements during one year. The expected value for this reference material is 0.710250 (see Faure and Mensing, 2005), which was used to renormalize $^{87}Sr/^{86}Sr$ of the samples on a daily basis. Strontium procedural blanks were <100 pg strontium and are negligible. Some of the samples were analyzed by solution MC–ICP–MS at the Curt Engelhorn Center for Archaeometry, Mannheim. Measurements of the same sample aliquots for plant and snail specimens using the two techniques MC–ICP–MS and TIMS yielded $^{87}Sr/^{86}Sr$ agreeing within less than 0.00008.

The strontium content of the water samples was measured by ICP-OES, at the Institute of Geosciences, Mainz. Analytical precision – determined by repeated analyses of Roth ICP solution (Multi-Element Standard Solution for Surface Water Testing) – was better than 0.5% RSD (relative standard deviations, 1σ). The accuracy of the measurements was 101.2% recovery.

3.3. Statistical analysis

Non-parametric statistics were used to describe the $^{87}Sr/^{86}Sr$ distribution and to compare $^{87}Sr/^{86}Sr$ between groups. The structure of the data was visualized using Kernel Density Estimates (RSC, 2006). Differences in $^{87}Sr/^{86}Sr$ between sample types were examined by applying the two-tailed Mann–Whitney *U* test, performed with PAST (http://folk.uio.no/ohammer/past/). This test was preferred over the *t*-test because of the small sample sizes, important differences in sample sizes between groups and some heterogeneities between

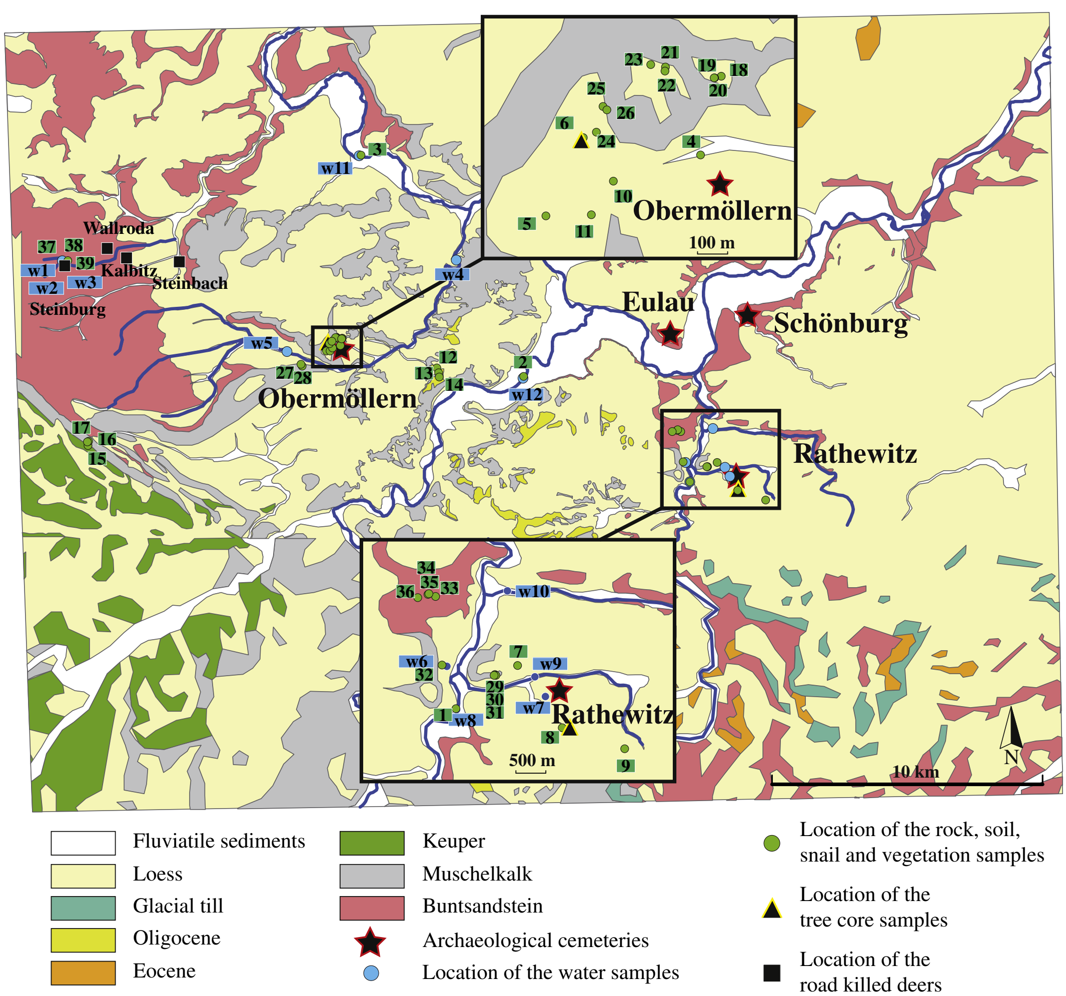

Fig. 2. Map of the geological bedrock from which the rock, soil, snail and vegetation (labels 1 to 39; data Table 1) and water (labels w1 to w12; data Table 2) samples were collected. The locations of the modern deer enamel (black squares) as well as the tree cores (black triangles) are also plotted.

variances. The null hypothesis states that there is no difference between the ranks of two samples. A probability level of 5% was considered significant to reject the null hypothesis. The probability was given by the exact p-value when $n1+n2 \leq 30$; otherwise, the asymptotic approximation p (same) was reported.

4. Results

4.1. $^{87}Sr/^{86}Sr$ of the different environmental materials

All results are listed in Tables 1 and 2. If not otherwise noted, errors are reported as $\pm 2\sigma$. The modern environmental samples collected within the region of Naumburg, central Germany, display a broad range in average $^{87}Sr/^{86}Sr$ ratios (Fig. 3). The soil leachates and water samples yield the highest mean values of 0.7103 ± 0.0022 and 0.7097 ± 0.0015, respectively, which are consistent with the average ratios measured in the archeological human bones and enamel, which are respectively 0.7099 ± 0.0006 and 0.7098 ± 0.0011 (data described in Knipper et al., 2012). The archeological faunal teeth data are slightly lower, averaging 0.7094 ± 0.0009, excluding two outliers. The least radiogenic modern material is represented by the deer enamel (0.7076 ± 0.0016). Intermediate values occur in plants – tree leaves and ground vegetation have 0.7094 ± 0.0015 and 0.7090 ± 0.0014, respectively – as well as in snail shells and rock leachates, which exhibit values of 0.7086 ± 0.0010 and 0.7083 ± 0.0015, respectively. Although plants yield fairly similar $^{87}Sr/^{86}Sr$ ratios, tree leaves are consistently more radiogenic than ground vegetation from the very same location (average difference in $^{87}Sr/^{86}Sr$: 0.0003 ± 0.0004; Fig. 4) whereas snail shells and rock leachates tend to yield lower $^{87}Sr/^{86}Sr$ ratios than ground vegetation (average difference in $^{87}Sr/^{86}Sr$: −0.0001 ± 0.0007 and −0.0004 ± 0.0009; respectively). The average intra-site difference in $^{87}Sr/^{86}Sr$ between ground vegetation and soil leachates is 0.0005 ± 0.0013.

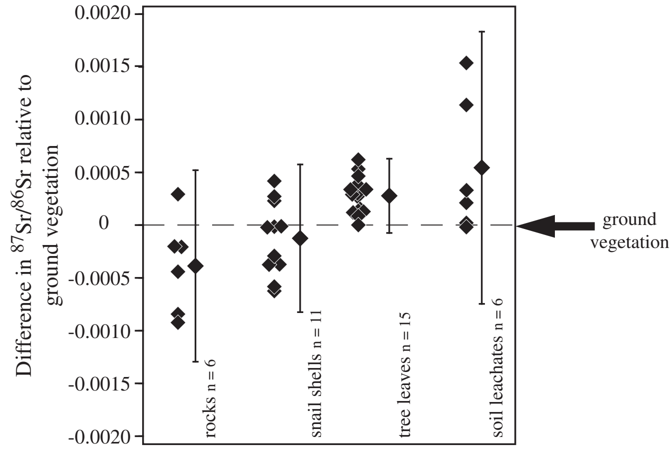

Fig. 4. Differences in $^{87}Sr/^{86}Sr$ ratios of rocks, snail shells, tree leaves and soil leachates relative to the ground vegetation collected at the same sampling location (cf. Table 1).

It is worth noting that for the tree leaves, the inter- and intra-species difference in $^{87}Sr/^{86}Sr$ is less than 0.0001 (Table 1; localities No. 8, No. 21 and No. 28, respectively). Two aliquots collected from the same rock (Table 1; locality No.17) also show fairly similar $^{87}Sr/^{86}Sr$ ratios (difference ≤ 0.0001).

4.2. $^{87}Sr/^{86}Sr$ of samples collected on different geological units

Considering all the samples collected on specific geological units (Fig. 5), the Middle Buntsandstein exhibits higher, although not significantly different, biologically-available $^{87}Sr/^{86}Sr$ values than those of the Upper Buntsandstein (average $^{87}Sr/^{86}Sr$: 0.7108 ± 0.0018 and 0.7099 ± 0.0005, respectively; Mann–Whitney $U=5$, $n1=5$, $n2=6$,

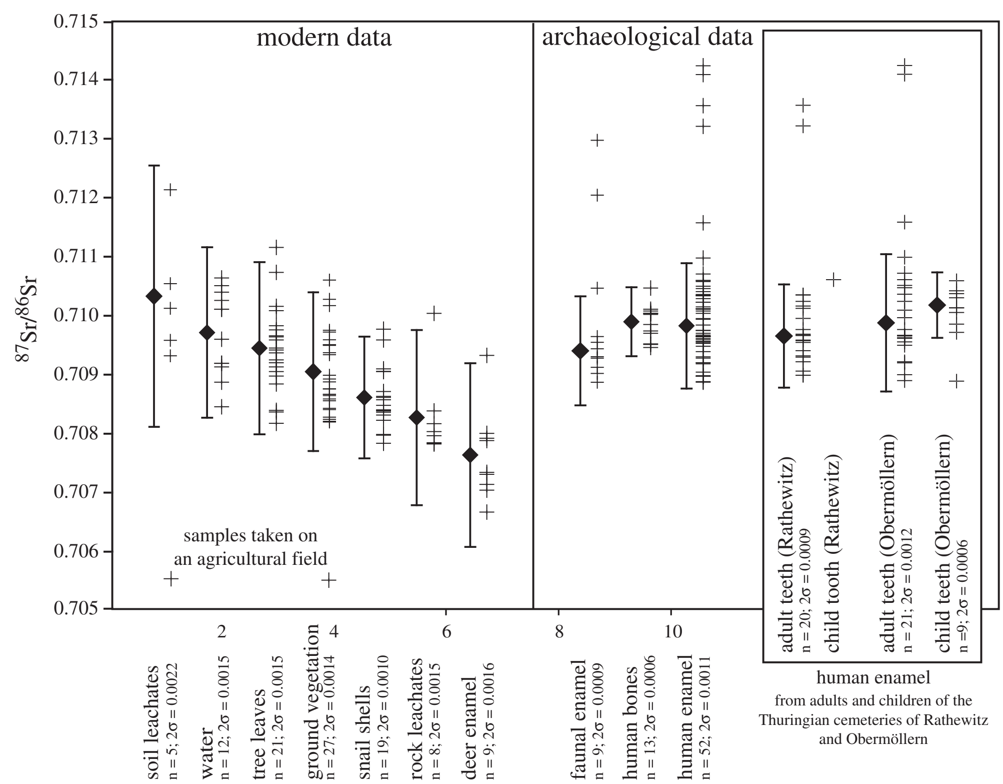

Fig. 3. Strontium isotope ratios of the archeological and modern, biological and geological samples collected in the vicinity of the Thuringian cemeteries. The $^{87}Sr/^{86}Sr$ of each sample within each sample category is shown (crosses). The regional average ± 2σ (diamonds plus bars) are provided for each kind of sample. The strontium isotopic compositions of the archeological human skeletons are also shown (Knipper et al., 2012).

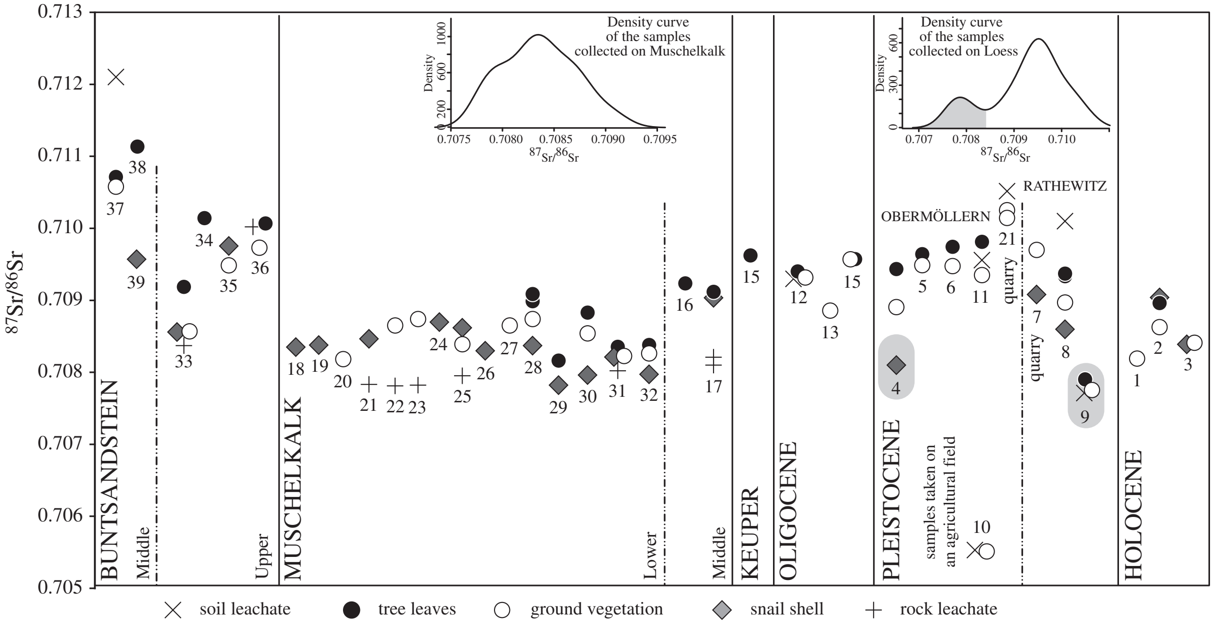

Fig. 5. Strontium isotope ratios of rocks (crosses), soils (oblique crosses), snail shells (diamonds), ground vegetation (white circle) and tree leaves (black circles) collected at each locality (numbered from 1 to 39, cf. Fig. 2). The data are sorted according to the geological units: Middle and Upper Buntsandstein, Lower and Middle Muschelkalk, Keuper, Oligocene, Pleistocene (loess) and Holocene (fluvial sediments). The graph is accompanied by kernel density plots of the $^{87}Sr/^{86}Sr$ of the samples collected on Muschelkalk and loess outcrops to show the principal mode of distribution of the values. The portion of the curve highlighted in gray represents data that were most likely contaminated (localities No. 4 and 9) and are therefore not included in the calculations.

P = 0.08, two-tailed). The samples directly collected on gypsum layers (Fig. 5; locality No. 33) from the Upper Buntsandstein display lower values (0.7087 ± 0.0007), which are slightly higher than those measured in samples collected on Muschelkalk (0.7084 ± 0.0008). The riverine sediments on average yield fairly similar $^{87}Sr/^{86}Sr$ ratios (0.7086 ± 0.0007). The samples collected on Pleistocene units (loess) yield intermediate values (0.7095 ± 0.0010), which differ significantly from those exhibited by the Middle Buntsandstein (Mann–Whitney $U = 7$, n1 = 17, n2 = 5, P = 0.003, two-tailed) and the Muschelkalk (Mann–Whitney $U = 21$, n1 = 17, n2 = 34, P (same) < 0.0001, two-tailed), which represent the $^{87}Sr/^{86}Sr$ end-members for bioavailable Sr in this region. The samples collected on Oligocene sediments provide similar values (0.7094 ± 0.0005) to those of the loess. Finally, the single sample collected on Keuper has a $^{87}Sr/^{86}Sr$ ratio of 0.7096.

4.3. $^{87}Sr/^{86}Sr$ through time (tree core and freshwater bivalve shells)

No significant difference in $^{87}Sr/^{86}Sr$ was observed between bivalve shell samples mineralized during early and late ontogeny (mean difference: 0.00003; Fig. 6). The archeological shells from locality A (Table 2) yield fairly homogeneous $^{87}Sr/^{86}Sr$ through archeological time (Middle Neolithic to Late Bronze Age: mean value 0.7084 ± 0.0001). The $^{87}Sr/^{86}Sr$ of Saale River water, sampled near the archeological site of Salzmünde, is 0.7087 (Table 2; sample w13) and therefore only differs by about 0.0003 from that of the bivalves. The archeological (Iron Age) and the modern (year 1997) shells from two adjacent localities, B and C, from the Helme River (Figs. 1 and 6), show comparable $^{87}Sr/^{86}Sr$ ratios (difference: 0.0003), which differ substantially from those of a recent shell (difference: 0.0019), collected at around 30 km further west in the same river (locality D, Fig. 6). Such a difference is also observed in the signature of their aquatic environments (difference: 0.0017). It is worth noting that the difference in $^{87}Sr/^{86}Sr$ ratios between the bivalves and their corresponding aquatic milieu lies between 0.0001 (for localities B and C) and 0.0002 (locality D).

The tree core sampled near to Rathewitz recorded decreasing $^{87}Sr/^{86}Sr$ values from 1925–1930 (0.7110) to 1970–1975 (0.7094) (Fig. 7). From then to modern times, the $^{87}Sr/^{86}Sr$ remains fairly constant (mean value 0.7094 ± 0.0001). The tree core sampled close to the locality of Obermöllern displays a similar decreasing trend, but with overall lower values (from 0.7100 to 0.7092) and one "outlier" (0.7102 in 1970–1975) from the trend observed from 1960 to 1965 onwards (0.7093 ± 0.0001).

A soil core (Table 1; locality No. 8) was taken 30 m away from the Rathewitz tree core on loess cover. The four soil samples analyzed from the soil core display highly variable $^{87}Sr/^{86}Sr$: from 0.70884 (humus layer) to 0.71478 (sandy mineral soil at the bottom of the core, 60 cm depth).

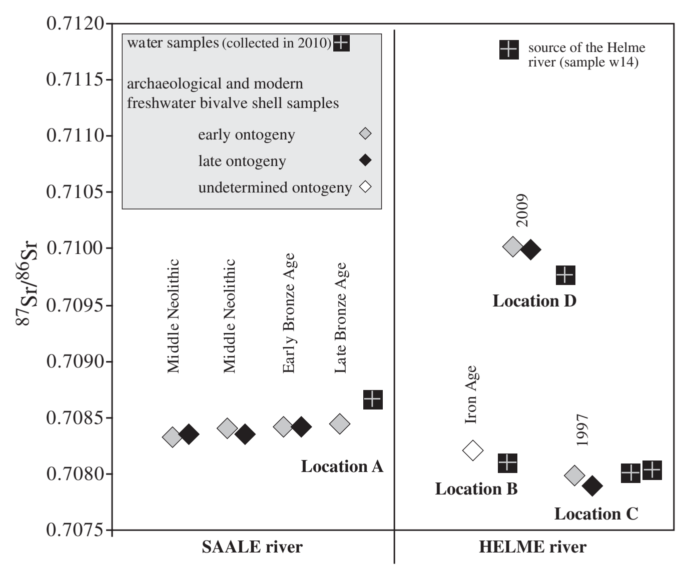

Fig. 6. Strontium isotope ratios of archeological and modern freshwater bivalve shells from the Saale and Helme rivers. Samples from shell parts formed during early and late ontogeny of each bivalve are plotted (diamonds), along with those of their aquatic milieu (squares). Locations (A to D, cf. Fig. 1) and time of collection (from Middle Neolithic to 2009) are reported next to each data point.

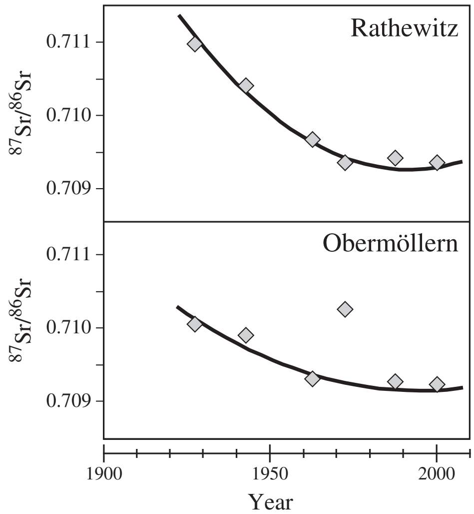

Fig. 7. Strontium isotopic compositions of samples from two modern tree cores (from oaks) from near the localities Obermöllern and Rathewitz. The $^{87}Sr/^{86}Sr$ were obtained on tree rings averaging 5 years each, from 1925–1930 to 1998–2003. A decreasing trend in $^{87}Sr/^{86}Sr$ over time is observed in both tree cores.

5. Discussion

5.1. Geological vs. biological-available Sr

The weathering of bedrock is certainly heterogeneous, with radiogenic Sr usually preferentially mobilized (Blum et al., 1993; Blum and Erel, 1997; Erel et al., 2004). The soil will also likely contain primary mineral fragments of the least-weatherable basement minerals, as well as newly-formed clays and carbonates. Altogether, bedrock minerals, soils and pore waters will be heterogeneous in $^{87}Sr/^{86}Sr$, which will reflect a complex balance between weathering rates, the age of the weathering surface as well as the geological age of the substrate. Soils on geologically "old" basement terrains are expected to exhibit the most extreme variation in $^{87}Sr/^{86}Sr$ ratios (see Blum and Erel, 1997).

This geological and pedological setting dictates the dispersion in $^{87}Sr/^{86}Sr$, which is then somehow pooled and assimilated into the so-called "bioavailable Sr" entering the food chain and, ultimately, humans and animals. Depending on what material one uses as a monitor of bioavailable Sr, the natural $^{87}Sr/^{86}Sr$ variations will either be homogenized or, perhaps, skewed towards a particular reservoir of strontium in the environment. It is the purpose, here, to shed light on what materials would be best to use in this regard, given that there is no consensus at all in the current literature in this regard.

5.2. Regional reference samples to use in mobility and migration studies

5.2.1. Modern vs. archeological faunal teeth $^{87}Sr/^{86}Sr$

It has been suggested that $^{87}Sr/^{86}Sr$ of deer teeth may be potential provenance indicators (Kierdorf et al., 2008), as some deer have relatively small roaming ranges of less than 70–80 ha (Kierdorf et al., 1999). Chemical compositions of deer teeth have also been used to monitor environmental pollution (Kierdorf et al., 1999; Kierdorf and Kierdorf, 1999; Richter et al., 2011). However, the deer teeth analyzed in this study clearly do not reflect the bioavailable $^{87}Sr/^{86}Sr$ of the unperturbed "natural" ecosystem. Measured $^{87}Sr/^{86}Sr$ ratios in the deer teeth are generally lower than 0.708, while water, soil, vegetation and snails collected on all of the geological substrates from the study area are mostly higher, lying between 0.708 and 0.710 (Fig. 3). $^{87}Sr/^{86}Sr$ measured on samples collected from an agricultural field (0.7055 measured in ground vegetation and soil leachate from locality No. 10, Table 1) illustrate that agricultural fertilizers (used in this region over the past decade) yield lower values than the marine carbonates of the Muschelkalk, which are the least radiogenic geological end-member of the study area (cf. Section 4.2). Such low strontium isotope values are usually measured in young mantle-derived volcanic rocks, which are not known to occur within approximately 50 km radius around the site (Fig. 1). Therefore, although modern fertilizers differ widely in their strontium isotopic composition, ranging from 0.7034 to 0.7152 (Vitoria et al., 2004), the unexpectedly low $^{87}Sr/^{86}Sr$ ratios of the deer enamel samples very likely result from the ingestion of food or water affected by unradiogenic fertilizers. Based on $^{87}Sr/^{86}Sr$ measured in a deer enamel sample from the locality of Steinburg (cf. Table 2, Fig. 2) mostly surrounded by Middle Buntsandstein in the deer roaming range area, the consumption of agricultural fertilized products would have accounted for 30% to the deer diet, assuming similar Sr/Ca ratios for woodland and agricultural plain plants. This is not an incongruous result despite the fact that roe deer is mainly a woodland species (Hewison et al., 2001), because deer also select weed species amongst crops in small woodlands and agricultural areas (Johnson, 1984; Putman, 1986). An important conclusion from our study is that modern faunal samples cannot be used unambiguously to determine the "baseline" for bioavailable $^{87}Sr/^{86}Sr$ in past migration studies in areas where fertilizers use has been documented.

In contrast, archeological faunal samples, which are free from anthropogenic contamination, should be the best archive for local bioavailable $^{87}Sr/^{86}Sr$, if the animals fed locally in the same area as the humans (Bentley, 2006; Price et al., 2002). Unfortunately, in this specific context, the statistical comparison of the clustered $^{87}Sr/^{86}Sr$ of archeological faunal teeth (Table 2, Fig. 3) with those of the $^{87}Sr/^{86}Sr$ data of archeological human teeth excavated in the same area (Knipper et al., 2012) implies different feeding areas for the fauna and the humans (two-tailed Mann–Whitney $U=76$, $n1=8$ $n2=52$, $P=0.004$; considering the major mode of human $^{87}Sr/^{86}Sr$, Fig. 9). Although this may lead to useful new questions regarding the way of life of past populations, this result justifies the examination of other environmental samples collected in the same ecosystem, in order to delimitate a "local signature" for investigating past migration, and opens the debate on their potential anthropogenic contamination.

5.2.2. Water samples

5.2.2.1. Strontium sources of the rivers analyzed. The strontium in water and thus $^{87}Sr/^{86}Sr$ of water mostly comes from the products of mineral weathering and atmospheric deposition (e.g. Bain and Bacon, 1994; Capo et al., 1998). Climate and, seasonality, which influences catchment discharge, also control the $^{87}Sr/^{86}Sr$ ratios of rivers (e.g. Land et al., 2000; Palmer and Edmond, 1989). Assessing the $^{87}Sr/^{86}Sr$ and Sr content of waters together is helpful in identifying the main lithologies from which the strontium isotopic composition of the water has been derived (e.g. Frei and Frei, 2011). If $^{87}Sr/^{86}Sr$ versus 1/Sr content yields a straight line, the isotopic composition of the water must be controlled by weathering of just two end-members. This is clearly illustrated by the samples collected from the Helme River (Fig. 8). Here, the $^{87}Sr/^{86}Sr$ is governed by the Lower Buntsandstein (radiogenic end-member), and most likely, evaporites from the Zechstein (unradiogenic end-member), which are found close to the river (Fig. 1).

All of the other water samples, which were mostly collected in the vicinity of the cemeteries, suggest simple binary mixing relationships. In this case, marine carbonates of the Muschelkalk are most likely the least radiogenic end-member, while the radiogenic $^{87}Sr/^{86}Sr$ end-member remains uncertain (see Fig. 8). The mixing line defined by these water samples seems to converge towards the same radiogenic end-member as that of the Helme River samples. However, the Lower Buntsandstein does not outcrop near the cemeteries, and it is therefore unlikely that this geological unit could supply radiogenic Sr to

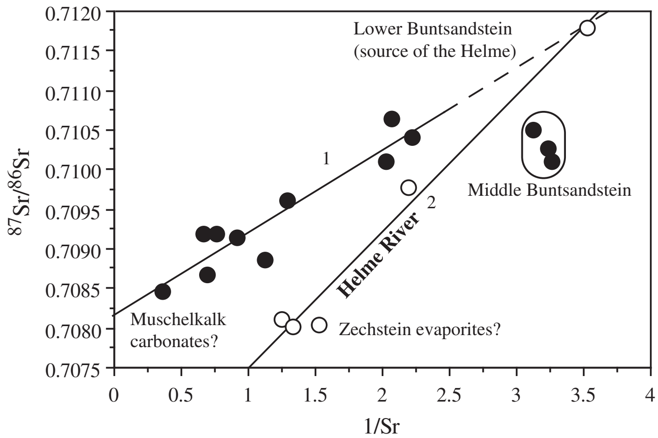

Fig. 8. $^{87}Sr/^{86}Sr$ vs. 1/Sr content (see data Table 2) of the water samples analyzed in this study. Two mixing lines are apparent: 1) the samples collected from the surroundings of the cemeteries (black circles), and 2) water samples from the Helme River (white circles). Both lines converge toward $^{87}Sr/^{86}Sr$ measured near the source of the Helme, which is located on Lower Buntsandstein. Water samples collected from a Middle Buntsandstein area have been excluded from the first mixing line.

streams and rivers from this area. According to the $^{87}Sr/^{86}Sr$ measured here for the geological units in this region, and inferred from the other samples analyzed, the Middle Buntsandstein is expected to have the highest overall $^{87}Sr/^{86}Sr$ ratio. However, the water samples collected directly at or close to a spring coming from Middle Buntsandstein outcrops have $^{87}Sr/^{86}Sr$ ratios that do not fall on the expected mixing line (Fig. 8). Whether this is due to anthropogenic contamination of the water or local differences in lithology remains to be investigated.

5.2.2.2. Anthropogenic contamination of the rivers?. Biogenic carbonates, such as bivalve shells, record the $^{87}Sr/^{86}Sr$ ratio of the dissolved Sr in the aquatic environment (Nakano and Hiroshi, 1991; Veizer, 1989), which itself is derived from weathering, atmospheric inputs, and anthropogenic activities in some cases (Christian et al., 2011). If the Sr inputs deviated from their long-term average, this would have modified the $^{87}Sr/^{86}Sr$ of the water, and this change would, in turn, be recorded in the sequential layers of mineralized carbonate during the growth of the bivalve shell (Åberg, 1995). Such changes over a short period of time (between 5 and 20 years) apparently did not occur, because very similar $^{87}Sr/^{86}Sr$ ratios are found in early- and late-formed ontogenetic portions of modern and archeological Unionidae shells (Fig. 6, Table 2). Likewise, changes over long periods of time (around 2000 years) can probably be excluded, since $^{87}Sr/^{86}Sr$ values of archeological shells from Salzmünde (locality A) are similar. This assumes, of course, that all the shells were collected from the same location by people and that they were not affected by later diagenetic processes (see cathodoluminescence investigations; Beierlein, 2011). The nearest river (Saale) has been suggested as the most probable collection site for the shells. A water sample (Table 2, w13) provides a slightly higher $^{87}Sr/^{86}Sr$ ratio (+0.0003) than that of the archeological shells. However, the exact provenance of the archeological shells is unknown, and might also be located further north within the Saale River. The sedimentary facies varies along the course of the Saale, with larger proportions of carbonates downstream (Hobert et al., 1994), thus the river water $^{87}Sr/^{86}Sr$ is expected to be lower further northward. This is illustrated by the difference of −0.0002 in the $^{87}Sr/^{86}Sr$ ratios between two water samples, w12 and w13, collected from the Saale further south and north, respectively. A modern shell (collected in 2009, locality D) also displays a slightly different $^{87}Sr/^{86}Sr$ (+0.0002) than the Helme River from which it was collected (Fig. 6). In contrast, an archeological shell from the Iron Age, which very likely came from the same river, exhibits a smaller difference (+0.0001) compared to that of the modern river water.

In summary, our $^{87}Sr/^{86}Sr$ data therefore suggest that although anthropogenic contamination of the Saale River has been reported (Zerling et al., 2003), the $^{87}Sr/^{86}Sr$ ratio was probably not affected significantly. Modern river waters in this region can therefore be used as comparative samples in studies of past mobility and migration. However, rivers drain diverse bedrock geology, that are spatially limited and variable. For this reason, using river waters alone as a reference point for bioavailable $^{87}Sr/^{86}Sr$ ratios would appear to be unwise.

5.3. Local reference samples to use in mobility and migration studies

To investigate the mobility of humans or animals using Sr isotope analysis of skeletal remains, the bioavailable $^{87}Sr/^{86}Sr$ needs to be characterized by appropriate environmental samples collected from each geological substratum in the presumed habitat. However, significant $^{87}Sr/^{86}Sr$ differences were observed in this study between different types of modern environmental samples collected in a restricted region. This raises serious questions about whether the so-called "local signature" can be easily and reliably determined from just a few samples, that are supposed to then represent the "baseline" for investigating past migrations.

5.3.1. Soil leachates

The $^{87}Sr/^{86}Sr$ values of the soil leachates illustrate just how poor this material is in providing an accurate estimate for the local $^{87}Sr/^{86}Sr$ signature. At the "regional scale", the soil leachates exhibit more variable $^{87}Sr/^{86}Sr$ ratios than that of all the other modern environmental samples (Fig. 3); similarly at a very local level (the same sites) the leachates provide values that are quite often inconsistent with the plant data (Fig. 4). Several studies have compared soil and plant $^{87}Sr/^{86}Sr$ ratios from the same locations (Blum et al., 2000; Evans and Tatham, 2004; Hodell et al., 2004; Nakano et al., 2001; Pett-Ridge et al., 2009; Poszwa et al., 2004). However, in those studies, the soil-exchangeable cations were obtained using various chemical reagents, which hampers direct comparison with our results — here we simply used MilliQ water. Nonetheless, Evans and Tatham (2004) did find discrepancies between the $^{87}Sr/^{86}Sr$ ratios of the soil leachates and vegetation as well, with slightly lower values occurring in the soils (average difference: 0.0002); this is the opposite of what we found here. Thus, it is clear that soils should only be used with caution for determining the bioavailable $^{87}Sr/^{86}Sr$, as they do not appear to yield consistent or reasonable comparative values.

5.3.2. Snail shells

Likewise, snail shells give a biased estimate of the bioavailable $^{87}Sr/^{86}Sr$. Evans et al. (2010) found that the $^{87}Sr/^{86}Sr$ recorded by snail shells appears to be shifted towards that of rainwater. Furthermore, land snails also incorporate significant amounts of soil carbonates into their diet — up to 40% (Yanes et al., 2008). As a result, snail shell $^{87}Sr/^{86}Sr$ are usually biased towards values for soil carbonates, which also seems to be the case for the snail shells analyzed in this study. Together, these observations strongly suggest that snail shells are unsuitable for providing accurate estimates of biosphere $^{87}Sr/^{86}Sr$.

5.3.3. Vegetation

5.3.3.1. Different rooting depth, different $^{87}Sr/^{86}Sr$. The $^{87}Sr/^{86}Sr$ that ends up in vegetation ultimately results from weathering of bedrock, as well as atmospheric deposition of material from outside the region (Åberg et al., 1989; Graustein and Armstrong, 1983; Nakano et al., 2001; Poszwa et al., 2004). As nutrient assimilation by the plant from the soil is affected by plant anatomy (root systems) as well as plant physiology (e.g., Sr cycling), which vary according to the species of plant (Poszwa et al., 2004), it is not altogether surprising to observe differences in $^{87}Sr/^{86}Sr$ between that of ground vegetation and that found in tree leaves. This difference is the same order of magnitude as that documented between bamboo grass and oaks in Japan (Nakano et al., 2001), and is slightly lower than that found between plantlet/young and mature trees in Belgium (Drouet et al., 2005a). Furthermore, the $^{87}Sr/^{86}Sr$ of the exchangeable Sr often varies between soil horizons (Drouet et al., 2007; Poszwa et al., 2002, 2004), as also indicated by the soil core data presented here, and thus plant-assimilated $^{87}Sr/^{86}Sr$ may vary according to rooting depth (Nakano et al., 2001; this study). The $^{87}Sr/^{86}Sr$ of a soil profile depends, among other parameters (see Pett-Ridge et al., 2009), on the weathering of the parent material (Drouet et al., 2007). However, the fact that $^{87}Sr/^{86}Sr$ of the intra-site ground vegetation is lower than that of the corresponding tree leaves reflects the overall lower $^{87}Sr/^{86}Sr$ found in top soils, which seems to occur regardless of the nature of the geological substrate. Although vegetation samples have been used as Sr isotope biosphere proxy (Evans et al., 2010; Kusaka et al., 2011), the constantly less radiogenic $^{87}Sr/^{86}Sr$ found in ground vegetation needs to be better understood. In particular, one must determine which type of plant, ground vegetation or tree leaves, yields the most reliable estimate of the bioavailable $^{87}Sr/^{86}Sr$ entering the food chain today and in the past.

5.3.3.2. Tree core samples: witness of environmental acidification?. In addition to ground vegetation and tree leaves, two tree cores were collected nearby each archeological cemetery. Both cores, sampled from oaks on loess outcrops, have quite similar $^{87}Sr/^{86}Sr$ ratios, but were quite variable over the last century (up to 0.0016 within the same tree). There is a trend of decreasing $^{87}Sr/^{86}Sr$ values towards recent times as can be seen in Fig. 7. This trend might be caused by years of mining activities. The Saale–Elbe region is known for its former coal mining industry (Eissmann, 2002), and anthropogenically-influenced groundwater has the lowest $^{87}Sr/^{86}Sr$ ratios in the Bitterfeld/Wolfen mining area (Petelet-Giraud et al., 2007), located 70 km away from our study area. Moreover, forests have been frequently limed in Germany, and especially during the 1980s (Huettl and Zoettl, 1993). The liming of forests can readily account for the decreasing trend in $^{87}Sr/^{86}Sr$ observed in a tree core (Drouet et al., 2005a) when the $^{87}Sr/^{86}Sr$ ratio of the underlying geological substrate is higher than that of the lime. However, if such local causes (mining activities and/or liming forests) are able to explain the decreasing $^{87}Sr/^{86}Sr$ values recorded in the tree cores, it is still difficult to establish any temporal link to such events due to the radial and vertical translocation of cations within trees themselves (Drouet et al., 2005a; Hagemeyer, 1993).

Besides the mining industry and lime addition, anthropogenic SO_2 emissions, mainly from coal burning over the last century, are also responsible for a decreasing trend in $^{87}Sr/^{86}Sr$ seen universally in tree ring samples from different areas, though the pattern of the decrease does vary according to the substrate and the tree species (Drouet et al., 2005a). Soil acidification leads to calcium depletion of the soil, and thus increases the relative contribution of atmospherically deposited Sr (Drouet et al., 2005a), which shifts the final $^{87}Sr/^{86}Sr$ of the vegetation. The dramatic damage in Scandinavia due to acid rain (Menz and Seip, 2004) might help explain the very high variability in $^{87}Sr/^{86}Sr$ measured by Åberg (1995) within a single oak tree in Stockholm. Evidence for mining, liming and/or soil acidification, all resulting from human activities, might be observable in the tree cores sampled near Naumburg, and are very likely responsible for the differences found in $^{87}Sr/^{86}Sr$ between ground vegetation and tree leaves. If this is indeed correct, then the $^{87}Sr/^{86}Sr$ of modern vegetation diverges from that of the past. Hence, it would be inappropriate to use modern vegetation as an archive for the local “biosignal” for comparison with $^{87}Sr/^{86}Sr$ of medieval skeletons excavated in the same area.

5.3.3.3. Statistics of $^{87}Sr/^{86}Sr$ in modern vegetation and archeological human teeth. A kernel density plot of $^{87}Sr/^{86}Sr$ measured in teeth of individuals buried in the area shows two major distribution modes, lying both between 0.708 and 0.711, and a few minor modes at higher $^{87}Sr/^{86}Sr$ (Fig. 9). If the population lived locally, these major modes most likely record bioavailable loess $^{87}Sr/^{86}Sr$, as loess dominates the landscape in the vicinity of each cemetery (Fig. 2). However, the ground vegetation $^{87}Sr/^{86}Sr$ do not support such an interpretation when compared to the archeological human dataset. The statistical probability that loess provided most of the dietary bioavailable Sr to the Thuringian population is less than 33% while for the Upper Buntsandstein the probability is higher than 60% for data from both cemeteries (Fig. 10). This statistical inference, however, is not supported by the sparsity of Upper Buntsandstein units in the vicinity of the cemeteries. Therefore, $^{87}Sr/^{86}Sr$ measured in ground vegetation and those of archeological human teeth do not provide a coherent or consistent picture of the bioavailable $^{87}Sr/^{86}Sr$ within the geological context of the region.

Fig. 10 shows that the bioavailable $^{87}Sr/^{86}Sr$, as recorded in the archeological human teeth, are in better overall agreement with the loess-hasted leaf data (probability of 56% and 86% for the adults buried in Obermöllern and Rathewitz, respectively). Nevertheless, the $^{87}Sr/^{86}Sr$ data for children buried in Obermöllern are, paradoxically, inconsistent with $^{87}Sr/^{86}Sr$ from loess, and are matched better by the signature seen in tree leaves collected on Upper Buntsandstein.

In summary, the fact that it is proving so difficult to arrive at a meaningful Sr isotope biosignature is perplexing. The most important aspect of our study is that we have analyzed Sr isotopes in so many diverse materials from this setting for $^{87}Sr/^{86}Sr$ to compare with $^{87}Sr/^{86}Sr$ data from the human population of ca. 1500 years ago from the region. The data illustrate the potential, but also the pitfalls, of many proxies of

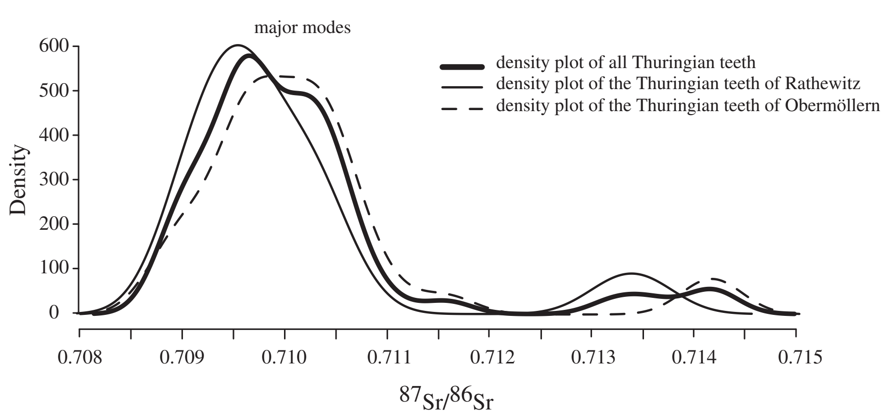

Fig. 9. Kernel density plots of Thuringian teeth $^{87}Sr/^{86}Sr$ of individuals buried in the cemeteries of Obermöllern and Rathewitz. The human $^{87}Sr/^{86}Sr$ are mainly distributed according to two major modes, which lie between 0.708 and 0.711. A few minor modes exist beyond 0.711 and up to 0.715.

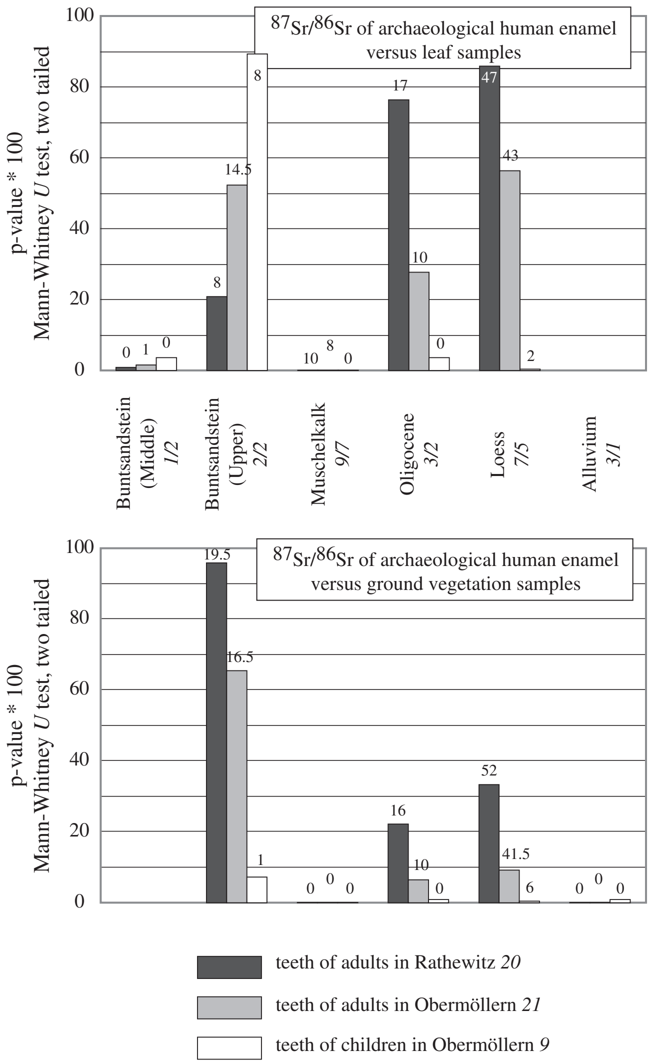

Fig. 10. Probability histogram of matching $^{87}Sr/^{86}Sr$ in teeth of 5–6th century AD Thuringian individuals and $^{87}Sr/^{86}Sr$ of different geological units found in the region, and as inferred from tree leaves (top) and ground vegetation (bottom) samples. The non-parametric statistical Mann–Whitney *U* test is applied to adult teeth of the Thuringian cemeteries of Obermöllern and Rathewitz and to tooth enamel samples of children buried in Obermöllern. The probability is given in % (P value ∗ 100, two-tailed Mann–Whitney *U* test) and the *U* value is reported on top of each sample group. The number of archeological or environmental samples (provided as a/b for each geological unit with (a) ground vegetation and (b), tree leaves) used in the calculation is given in italics.

bioavailable environmental $^{87}Sr/^{86}Sr$ used in the current archeological literature. It is clear that there is no one ideal material to use in this respect, and the choice is probably best made on a case-by-case basis, to avoid misleading inferences in past migration studies.

6. Conclusion

Archeological studies of past human migrations using Sr isotopes rely on a comparison of $^{87}Sr/^{86}Sr$ in skeletal remains with that of bioavailable Sr from the local surroundings. Many sorts of material have been used previously to estimate $^{87}Sr/^{86}Sr$ of bioavailable Sr, and it remains unclear which of these are appropriate or reliable. Here we measured the $^{87}Sr/^{86}Sr$ of a large number of different types of samples (water, soil leachate, snail shells, deer enamel, ground vegetation, tree leaves) from central Germany in order to infer which might be the best proxy for local bioavailable Sr in archeological studies. These data were compared with $^{87}Sr/^{86}Sr$ from bones and teeth of two 5–6th century AD cemeteries.

Our study demonstrates the influence of anthropogenic activities (e.g. fertilizers) on the $^{87}Sr/^{86}Sr$ of modern deer enamel and the $^{87}Sr/^{86}Sr$ of archeological faunal teeth (pigs, sheep/goat, and cattle) indicate that they fed in isotopically different areas than the Thuringian population. This justifies the investigation of environmental samples in order to provide a reliable $^{87}Sr/^{86}Sr$ baseline for investigating past migration. Among them, snail shells and soil leachates $^{87}Sr/^{86}Sr$ do not provide accurate estimates of that of bioavailable Sr. Rather, modern water and vegetation – especially tree leaves – appear to be the best suited materials to use, and most closely reflect $^{87}Sr/^{86}Sr$ of the local biosphere. The influence of anthropogenic activities on the $^{87}Sr/^{86}Sr$ of water and vegetation can be examined back in time using archives such as freshwater bivalve shells and tree cores, respectively. Modern and archeological bivalve shells rule out any significant deviation in $^{87}Sr/^{86}Sr$ of modern versus historic water samples. However, $^{87}Sr/^{86}Sr$ in tree ring cores exhibit a decreasing trend, indicative of anthropogenic influence on vegetation in the 20th century. This most likely results from mining, forest liming and/or soil acidification.

Comparison of the modern vegetation $^{87}Sr/^{86}Sr$ data with that of enamel from "Thuringian" skeletons suggests that the modern ground vegetation data are too unradiogenic as a consequence of anthropogenic effects. Data from tree leaves may also have been affected, but to a lesser extent.

Consequently, the results obtained in this study may be used as a recommendation for investigating movements of past populations, although very different results might arise in other areas. Overall, reference samples to reconstruct bioavailable $^{87}Sr/^{86}Sr$ for ancient humans and animals and infer their mobility, must be carefully selected considering factors such as anthropogenic influences on modern ecosystems, rooting depth of plants, as well as food sources used by modern and archeological fauna.

Acknowledgments

This work was financially supported by the BMBF (Bundesministerium für Bildung und Forschung). The authors thank Hans Joachim Döhle (Halle, Germany) as well as the Forestry Office of Sachsen-Anhalt for providing the archeological faunal teeth and the modern deer teeth, respectively. Michael Brauns, Sigrid Klaus and Bernd Höppner (Curt-Engelhorn Center of Archaeometry, Mannheim) analyzed a part of the samples. Ingrid Raczek, Heinz Feldmann and Gerlinde Borngässer (MPI, Mainz), as well as Michael Maus (Institute of Geosciences, Mainz) provided valuable analytical help and advice. Thanks go also to Lars Heller and Stefanie Thiele who helped in sample preparation. Wafa Abouchami is also acknowledged for decisive comments and secretarial assistance. Finally, we thank two anonymous reviewers who helped in improving the clarity of the manuscript.

References

Åberg G. The use of natural strontium isotopes as tracers in environmental studies. Water Air Soil Pollut 1995;79:309–22.
Åberg G, Jacks G, Hamilton PJ. Weathering rates and $^{87}Sr/^{86}Sr$ ratios: an isotopic approach. J Hydrol 1989;109:65–78.
Almeida CM, Vasconcelos MTSD. ICP-MS determination of strontium isotope ratio in wine in order to be used as a fingerprint of its regional origin. J Anal At Spectrom 2001;16:607–11.
Bain DC, Bacon JR. Strontium isotopes as indicators of mineral weathering in catchments. Catena 1994;22:201–14.
Barbaste M, Robinson K, Guilfoyle S, Medina B, Lobinski R. Precise determination of the strontium isotope ratios in wine by inductively coupled plasma sector field multicollector mass spectrometry (ICP–SF–MC–MS). J Anal At Spectrom 2002;17:135–7.
Beard BL, Johnson CM. Strontium isotope composition of skeletal material can determine the birth place and geographic mobility of humans and animals. J Forensic Sci 2000;45:1049–61.
Beierlein, L. High-resolution climate archives from archaeological sites in Central Germany. Diploma Thesis 2011.
Bentley RA. Strontium isotopes from the Earth to the archaeological skeleton: a review. J Archaeol Method Theory 2006;13:135–87.

Bentley RA, Price TD, Lüning J, Gronenborn D, Wahl J, Fullagar PD. Prehistoric migration in Europe: strontium isotope analysis of early Neolithic skeletons. Curr Anthropol 2002;43:799–804.

Bentley RA, Krause R, Price TD, Kaufmann B. Human mobility at the early Neolithic settlement of Vaihingen, Germany: evidence from strontium isotope analysis. Archaeometry 2003;45:471–86.

Bentley RA, Price TD, Stephan E. Determining the local $^{87}Sr/^{86}Sr$ range for archaeological skeletons: a case study from Neolithic Europe. J Archaeol Sci 2004;31:365–75.

Blum JD, Erel Y. Rb–Sr isotope systematics of a granitic soil chronosequence: the importance of biotite weathering. Geochim Cosmochim Acta 1997;61:3193–204.

Blum JD, Erel Y, Brown K. $^{87}Sr/^{86}Sr$ ratios of Sierra Nevada stream waters: implications for relative mineral weathering rates. Geochim Cosmochim Acta 1993;58: 5019–25.

Blum JD, Taliaferro EH, Weisse MT, Holmes RT. Changes in Sr/Ca, Ba/Ca and $^{87}Sr/^{86}Sr$ ratios between trophic levels in two forest ecosystems in the northeastern USA. Biogeochemistry 2000;49:87-101.

Blum JD, Taliaferro EH, Holmes RT. Determining the sources of calcium for migratory songbirds using stable strontium isotopes. Oecologia 2001;126:569–74.

Böhlke JK, Horan M. Strontium isotope geochemistry of groundwaters and streams affected by agriculture, Locust Grove, MD. Appl Geochem 2000;15:599–609.

Britton K, Grimes V, Niven L, Steele TE, McPherron S, Soressi M, et al. Strontium isotope evidence for migration in late Pleistocene Rangifer: implications for Neanderthal hunting strategies at the Middle Palaeolithic site of Jonzac, France. J Hum Evol 2011;61:176–85.

Capo RC, Stewart BW, Chadwick OA. Strontium isotopes as tracers of ecosystem processes: theory and methods. Geoderma 1998;82:197–225.

Christian LN, Banner JL, Mack LE. Sr isotopes as tracers of anthropogenic influences on stream water in the Austin, Texas, area. Chem Geol 2011;282:84–97.

Comar CL, Russell RS, Wasserman RH. Strontium–calcium movement from soil to man. Science 1957;126:485–92.

Dasch EJ. Strontium isotopes in weathering profiles, deep-sea sediments, and sedimentary rocks. Geochim Cosmochim Acta 1969;33:1521–52.

Dijkstra FA, Van Breemen N, Jongmans AG, Davies GR, Likens GE. Calcium weathering in forested soils and the effect of different tree species. Biogeochemistry 2003;62:253–75.

Drouet T, Herbauts J, Demaiffe D. Long-term records of strontium isotopic composition in tree rings suggest changes in forest calcium sources in the early 20th century. Glob Chang Biol 2005a;11:1926–40.

Drouet T, Herbauts J, Gruber W, Demaiffe D. Strontium isotope composition as a tracer of calcium sources in two forest ecosystems in Belgium. Geoderma 2005b;126: 203–23.

Drouet T, Herbauts J, Gruber W, Demaiffe D. Natural strontium isotope composition as a tracer of weathering patterns and of exchangeable calcium sources in acid leached soils developed on loess of central Belgium. Eur J Soil Sci 2007;58:302–19.

Eissmann L. Tertiary geology of the Saale–Elbe region. Quat Sci Rev 2002;21:1245–74.

Erel Y, Blum JD, Roueff E, Ganor J. Lead and strontium isotopes as monitors of experimental granitoid mineral dissolution. Geochim Cosmochim Acta 2004;68: 4649–63.

Ericson JE. Strontium isotope characterization in the study of prehistoric human ecology. J Hum Evol 1985;14:503–14.

Evans JA, Tatham S. Defining "local signature" in terms of Sr isotope composition using a tenth-to twelfth-century Anglo-Saxon population living on a Jurassic clay-carbonate terrain, Rutland, UK. In: Pye K, Croft DJ, editors. Forensic geoscience: principles, techniques and applications, vol. 232. London: Geological Society of London, Special Publications; 2004. p. 237–48.

Evans JA, Montgomery J, Wildman G, Boulton N. Spatial variations in biosphere $^{87}Sr/^{86}Sr$ in Britain. J Geol Soc London 2010;167:1–4.

Faure G, Mensing TM. Isotopes: principles and applications. 3rd ed. New Jersey: John Wiley and Sons, Inc.; 2005.

Feranec RS, Hadly EA, Paytan A. Determining landscape use of Holocene mammals using strontium isotopes. Oecologia 2007;153:943–50.

Fortunato G, Mumic K, Wunderli S, Pillonel L, Bosset JO, Gremaud G. Application of strontium isotope abundance ratios measured by MC–ICP–MS for food authentication. J Anal At Spectrom 2004;19:227–34.

Frei KM, Frei R. The geographic distribution of strontium isotopes in Danish surface waters — a base for provenance studies in archaeology, hydrology and agriculture. Appl Geochem 2011;26:326–40.

Graustein WC. $^{87}Sr/^{86}Sr$ ratios measure the sources and flow of strontium in terrestrial ecosystems. In: Rundel PW, Ehleringer JR, Nagy KA, editors. Stable isotopes in ecological research. New-York: Springer-Verlag; 1989. p. 491–512.

Graustein WC, Armstrong RL. The use of strontium-87/strontium-86 ratios to measure atmospheric transport into forested watersheds. Science 1983;219:289–92.

Hagemeyer J. Monitoring trace metal pollution with tree rings: a critical reassessment. In: Markert B, editor. New York: VCH Weinheim; 1993. p. 541–63.

Hallmann N, Schöne BR, Strom A, Fiebig J. An intractable climate archive — sclerochronological and shell oxygen isotope analyses of the Pacific geoduck, *Panopea abrupta* (bivalve mollusk) from Protection Island (Washington State, USA). Palaeogeogr Palaeoclimatol Palaeoecol 2008;269:115–26.

Hewison AJM, Vincent JP, Joachim J, Angibault JM, Cargnelutti B, Cibien C. The effects of woodland fragmentation and human activity on roe deer distribution in agricultural landscapes. Can J Zool 2001;79:679–89.

Hobert H, Schultz U, Einax J. Characterization of Saale River sediments by IR spectroscopy. Acta Hydrochim Hydrobiol 1994;22:76–84.

Hodell DA, Quinn RL, Brenner M, Kamenov G. Spatial variation of strontium isotopes ($^{87}Sr/^{86}Sr$) in the Maya region: a tool for tracking ancient human migration. J Archaeol Sci 2004;31:585–601.

Hoppe KA, Koch PL. Reconstructing the migration patterns of late Pleistocene mammals from northern Florida, USA. Quat Res 2007;68:347–52.

Hoppe KA, Koch PL, Carlson RW, Webb SD. Tracking mammoths and mastodons: reconstruction of migratory behavior using strontium isotope ratios. Geology 1999;27: 439–42.

Huettl RF, Zoettl HW. Liming as a mitigation tool in Germany's declining forests — reviewing results from former and recent trials. For Ecol Manage 1993;61:325–38.

Johnson TH. Habitat and social organisation of roe deer (*Capreolus capreolus*). PhD Thesis, University of Southampton, 1984.

Juarez CA. Strontium and geolocation, the pathway to identification for deceased undocumented Mexican border-crossers: a preliminary report. J Forensic Sci 2008;53:46–9.

Kierdorf U, Kierdorf H. Dental fluorosis in wild deer: its use as a biomarker of increased fluoride exposure. Environ Monit Assess 1999;57:265–75.

Kierdorf H, Kierdorf U, Sedlacek F. Monitoring regional fluoride pollution in the Saxonian Ore mountains (Germany) using the biomarker dental fluorosis in roe deer (*Capreolus capreolus* L.). Sci Total Environ 1999;232:159–68.

Kierdorf H, Åberg G, Kierdorf U. Lead concentrations and lead and strontium stable-isotope ratios in teeth of European roe deer (*Capreolus capreolus*). Eur J Wildl Res 2008;54:313–9.

Knipper C, Maurer A-F, Peters D, Meyer C, Brauns M, Galer S, et al. Mobility in Thuringia or mobile Thuringians: a strontium isotope study from early Medieval central Germany. In: Burger J, Kaiser E, Schier W, editors. Population dynamics in pre- and early history: new approaches by using stable isotopes and genetics. Berlin: De Gruyter Inc.; 2012.

Knudson KJ, Price TD, Buikstra JE, Blom DE. The use of strontium isotope analysis to investigate Tiwanaku migration and mortuary ritual in Bolivia and Peru. Archaeom 2004;46:5-18.

Knudson KJ, Tung TA, Nystrom KC, Price TD, Fullagar PD. The origin of the Juch'uypampa Cave mummies: strontium isotope analysis of archaeological human remains from Bolivia. J Archaeol Sci 2005;32:903–13.

Kusaka S, Nakano T, Yumoto T, Nakatsukasa M. Strontium isotope evidence of migration and diet in relation to ritual tooth ablation: a case study from the Inariyama Jomon site, Japan. J Archaeol Sci 2011;38:166–74.

Land M, Ingri J, Andersson PS, Ohlander B. Ba/Sr, Ca/Sr and $^{87}Sr/^{86}Sr$ ratios in soil water and groundwater: implications for relative contributions to stream water discharge. Appl Geochem 2000;15:311–25.

Menz FC, Seip HM. Acid rain in Europe and the United States: an update. Environ Sci Policy 2004;7:253–65.

Montgomery J, Evans JA, Wildman G. $^{87}Sr/^{86}Sr$ isotope composition of bottled British mineral waters for environmental and forensic purposes. Appl Geochem 2006;21:1626–34.

Montgomery J, Evans JA, Cooper RE. Resolving archaeological populations with Sr-isotope mixing models. Appl Geochem 2007;22:1502–14.

Müller W, Fricke H, Halliday AN, McCulloch MT, Wartho J-A. Origin and migration of the Alpine Iceman. Science 2003;302:862–5.

Nafplioti A. Tracing population mobility in the Aegean using isotope geochemistry: a first map of local biologically available $^{87}Sr/^{86}Sr$ signatures. J Archaeol Sci 2011;38:1560–70.

Nakano T, Hiroshi N. Strontium isotopic equilibrium of limnetic molluscs with ambient lacustrine water in Uchinuma and Kasumigaura, Japan. Ann Rep Inst Geosci Univ Tsukuba 1991;17:52–5.

Nakano T, Yokoo Y, Yamanaka M. Strontium isotope constraint on the provenance of basic cations in soil water and stream water in the Kawakami volcanic watershed, central Japan. Hydrol process 2001;15:1859–75.

Nollet S, Koerner T, Kramm U, Hilgers C. Precipitation of fracture fillings and cements in the Buntsandstein (NW Germany). Geofluids 2009;9:373–85.

Palmer MR, Edmond JM. The strontium isotope budget of the modern ocean. Earth Planet Sci Lett 1989;92:11–26.

Petelet-Giraud E, Negrel P, Gourcy L, Schmidt C, Schirmer M. Geochemical and isotopic constraints on groundwater–surface water interactions in a highly anthropized site. The Wolfen/Bitterfeld megasite (Mulde subcatchment, Germany). Environ Pollut 2007;148:707–17.

Pett-Ridge JC, Derry LA, Barrows JK. Ca/Sr and $^{87}Sr/^{86}Sr$ ratios as tracers of Ca and Sr cycling in the Rio Icacos watershed, Luquillo Mountains, Puerto Rico. Chem Geol 2009;267:32–45.

Poszwa A, Dambrine E, Ferry B, Pollier B, Loubet M. Do deep tree roots provide nutrients to the tropical rainforest? Biogeochemistry 2002;60:97-118.

Poszwa A, Ferry B, Dambrine E, Pollier B, Wickman T, Loubet M, et al. Variations of bioavailable Sr concentration and $^{87}Sr/^{86}Sr$ ratio in boreal forest ecosystems. Role of biocycling, mineral weathering and depth of root uptake. Biogeochemistry 2004;67:1-20.

Price TD, Manzanilla L, Middleton WD. Immigration and the ancient city of Teotihuacan in Mexico: a study using strontium isotope ratios in human bone and teeth. J Archaeol Sci 2000;27:903–13.

Price TD, Burton JH, Bentley RA. The characterization of biologically available strontium isotope ratios for the study of prehistoric migration. Archaeom 2002;44:117–35.

Price TD, Tiesler V, Burton JH. Early African diaspora in colonial Campeche, Mexico: strontium isotopic evidence. Am J Phys Anthropol 2006a;130:485–90.

Price TD, Wahl J, Bentley RA. Isotopic evidence for mobility and group organization among Neolithic farmers at Talheim, Germany, 5000 BC. Eur J Archaeol 2006b;9: 259–84.

Putman RJ. Foraging by roe deer in agricultural areas and impact on arable crops. J Appl Ecol 1986;23:91–9.

Radloff FGT, Mucina L, Bond WJ, le Roux PJ. Strontium isotope analyses of large herbivore habitat use in the Cape Fynbos region of South Africa. Oecologia 2010;164: 567–78.

Richter H, Kierdorf U, Richards A, Melcher F, Kierdorf H. Fluoride concentration in dentine as a biomarker of fluoride intake in European roe deer (*Capreolus capreolus*) — an electron-microprobe study. Arch Oral Biol 2011;56:785–92.

Rosenthal HL, Cochran OA, Eves MM. Strontium content of mammalian bone, diet and excreta. Environ Res 1972;5:182–91.

RSC, Royal Society of Chemistry. AMC Technical Brief 4, representing data distributions with kernel density estimates; 2006. www.rsc.org/amc/.

Schweissing MM, Grupe G. Stable strontium isotopes in human teeth and bone: a key to migration events of the late Roman period in Bavaria. J Archaeol Sci 2003;30:1373–83.

Shand P, Darbyshire DPF, Love AJ, Edmunds WM. Sr isotopes in natural waters: applications to source characterisation and water–rock interaction in contrasting landscapes. Appl Geochem 2009;24:574–86.

Sillen A, Hall G, Richardson S, Armstrong R. $^{87}Sr/^{86}Sr$ ratios in modern and fossil food-webs of the Sterkfontein Valley: implications for early hominid habitat preference. Geochim Cosmochim Acta 1998;62:2463–73.

Swoboda S, Brunner M, Boulyga SF, Galler P, Horacek M, Prohaska T. Identification of Marchfeld asparagus using Sr isotope ratio measurements by MC–ICP–MS. Anal Bioanal Chem 2008;390:487–94.

Tafuri MA, Bentley RA, Manzi G, Lernia SD. Mobility and kinship in the prehistoric Sahara: strontium isotope analysis of Holocene human skeletons from the Acacus Mts. (southwestern Libya). J Anthropol Archaeol 2006;25:390–402.

Techer I, Lancelot J, Descroix F, Guyot B. About Sr isotopes in coffee 'Bourbon Pointu' of the Réunion Island. Food Chem 2011;126:718–24.

Tichomirowa M, Heidel C, Junghans M, Haubrich F, Matschullat J. Sulfate and strontium water source identification by O, S and Sr isotopes and their temporal changes (1997–2008) in the region of Freiberg, central-eastern Germany. Chem Geol 2010;276:104–18.

Toots H, Voorhies MR. Strontium in fossil bones and the reconstruction of food chains. Science 1965;149:854–5.

Tung TA, Knudson KJ. Social identities and geographical origins of Wari trophy heads from Conchopata, Peru. Curr Anthropol 2008;49:915–25.

Tütken T, Vennemann TW, Pfretzschner H-U. Nd and Sr isotope compositions in modern and fossil bones — proxies for vertebrate provenance and taphonomy. Geochim Cosmochim Acta 2011;75:5951–70.

Veizer J. Strontium isotopes in seawater through time. Annu Rev Earth Planet Sci 1989;17:141–67.

Vitoria L, Otero N, Soler A, Canals A. Fertilizer characterization: isotopic data (N, S, O, C and Sr). Environ Sci Technol 2004;38:3254–62.

Voerkelius S, Lorenz GD, Rummel S, Quétel CR, Heiss G, Baxter M, et al. Strontium isotopic signatures of natural mineral waters, the reference to a simple geological map and its potential for authentication of food. Food Chem 2010;118: 933–40.

West JB, Hurley JM, Dudas FO, Ehleringer JR. The stable isotope ratios of marijuana. II. Strontium isotopes relate to geographic origin. J Forensic Sci 2009;54:1261–9.

Wright LE. Identifying immigrants to Tikal, Guatemala: defining local variability in strontium isotope ratios of human tooth enamel. J Archaeol Sci 2005;32:555–66.

Yanes Y, Delgado A, Castillo C, Alonso MR, Ibáñez M, De la Nuez J, et al. Stable isotope ($\delta^{18}O$, $\delta^{13}C$, and δD) signatures of recent terrestrial communities from a low-latitude, oceanic setting: endemic land snails, plants, rain, and carbonate sediments from the eastern Canary Islands. Chem Geol 2008;249:377–92.

Zerling L, Hanisch C, Junge FW, Müller A. Heavy metals in Saale sediments. Changes in the contamination since 1991. Acta Hydrochim Hydrobiol 2003;31:368–77.

Ziegler PA. Geological atlas of western and central Europe. 2nd ed. Shell International Petroleum Maatschappij BV; 1990.